

DOI: <https://doi.org/10.31073/mivg202402-398>

Available at (PDF): <https://mivg.iwpim.com.ua/index.php/mivg/article/view/398>

UDC 631.67:004

## ASSESSMENT OF THE EVAPOTRANSPIRATION COMPONENTS DYNAMICS IN DIFFERENT AGRO-CLIMATIC ZONES OF UKRAINE USING THE PENMAN – MONTEITH – LEUNING MODEL

**T.V. Matiash<sup>1</sup>, Ph.D. in Technical Sciences, Ya.O. Butenko<sup>2</sup>, Ph.D. in Agricultural Sciences, A.M. Smirnov<sup>3</sup>, Ph.D. student, E.I. Matiash<sup>4</sup>, Master**

<sup>1</sup> Institute of Water Problems and Land Reclamation of NAAS, Kyiv, Ukraine; <https://orcid.org/0000-0003-1225-086X>; e-mail: [t.v.matiash@gmail.com](mailto:t.v.matiash@gmail.com);

<sup>2</sup> Institute of Water Problems and Land Reclamation of NAAS, Kyiv, Ukraine; <https://orcid.org/0000-0002-1743-7175>; e-mail: [iarynabulba@gmail.com](mailto:iarynabulba@gmail.com);

<sup>3</sup> Institute of Water Problems and Land Reclamation of NAAS, Kyiv, Ukraine; <https://orcid.org/0009-0006-5865-9141>; e-mail: [justtosha@gmail.com](mailto:justtosha@gmail.com);

<sup>4</sup> NTUU “Igor Sikorsky Kyiv Polytechnic Institute”, Kyiv, Ukraine; <https://orcid.org/0009-0007-7079-3017>; e-mail: [liza.mymailbox@gmail.com](mailto:liza.mymailbox@gmail.com)

**Abstract.** *The results of the assessment of evapotranspiration (ET) and its components based on remote sensing data are presented in the paper. To obtain this assessment, a special software was developed, namely the scripts using the JavaScript programming language for remote data processing in the Google Earth Engine (GEE) cloud software environment. This software allows to adjust the Penman – Monteith – Leuning (PML) model for the conditions of Ukraine and visualize the spatial distribution of ET. The usage of the cloud capabilities of the service made it possible to access the collection of images and carry out their remote processing using the Penman – Monteith – Leuning algorithm calibrated according to the data of the global network of eddy covariance monitoring stations. The result of such an assessment was a composite mosaic – a spatially distributed generalized image of evapotranspiration and its three main components: transpiration from vegetation ( $E_c$ ), evaporation from the soil ( $E_s$ ) and evaporation of precipitation intercepted by vegetation cover ( $E_i$ ) on the territory of Ukraine for the 2020 growing season. Understanding the dynamics of these components helps to optimize the water resources use and develop effective irrigation schemes, especially in the climate change conditions. As a result of the analysis of the evapotranspiration components' dynamics during the growing season, the most important component of evapotranspiration for different agro-climatic zones was determined.*

*However, the models, which are using remote data to estimate evapotranspiration dynamics, require additional validation and comparison with field measurements to improve their accuracy. Quantitative indicators obtained through modeling should be consistent with the data from ground-based greenhouse gas flows monitoring stations, which will contribute to the improvement of the methodology and its adaptation to the conditions of different agricultural regions. In addition, the use of the maps of geospatial distributed evapotranspiration allows to identify regions with increased transpiration and potential shortage of water resources. Such maps become a valuable tool for planning and forecasting water resources, which is critically important for the agricultural sector.*

**Key words:** *evapotranspiration, components of evapotranspiration, agro-climatic zones, remote sensing, soil-plant-atmosphere, information system, Penman – Monteith – Leuning model, PML-V2, GEE programming*

**Relevance of the research.** Actual evapotranspiration (ET) measured using remote sensing data, which includes transpiration from vegetation ( $E_c$ ), evaporation from soil ( $E_s$ ), and evaporation of intercepted precipitation by vegetation cover ( $E_i$ ), is the most important component of the energy balance in the “soil–plant–atmosphere” system [1]. ET and its components play a key role in linking ecosystem functioning, climate feedback, and water resources

[2]. Water consumption by agricultural crops is a critical parameter for water and energy exchange in agricultural production [3]. Understanding the dynamics and characteristics of crops' ET components has a great importance for the estimation of irrigation water needs [4], the evaluation of water use efficiency [5], and the design of optimal irrigation or drainage schemes [6].

Ground-based methods for the determination of components have not been widely applied

in scientific research mainly due to limitations related to time consumption, expensive equipment, and susceptibility to measurement manipulations and significant assumptions in calculations [7]. Therefore, great efforts have been made to disentangle ET and its components using independent approaches, namely the acquisition of datasets using satellite measurements and simulations with a major focus on improving the surface conductivity model based on the Penman – Monteith (PM) model. The improvement of this model included taking into account the stomatal conductivity of the reflected surface, that is the Penman – Monteith model as a result of Leuning’s improvement (PML) [2, 8, 9] received a connection with the vegetation located on the scanned surface and its productivity. The combination of the obtained results with the measurements of flows performed by the eddy covariance towers made it possible to obtain a relatively accurate set of global data.

Due to differences in climate, geomorphology, soil, hydrological regimes, and agricultural practices, ET components and the share of components for agricultural crops differ significantly depending on agro-climatic zones [2]. Evapotranspiration is a critical process and the most important component of the so-called “green” water cycle [10, 11]; and, therefore, the quantification of ET components and understanding of their dynamics can help in better and more efficient management of limited natural water resources, in spatial assessment and dissemination of local results, as well as in determining optimal zones for the use of natural water resources, determining optimal irrigation and drainage schemes. However, the changes and characteristics of ET components are still not fully understood and require further research. Therefore, this study was conducted to obtain information in the form of maps on the spatial distribution of evapotranspiration and its components depending on different agro-climatic zones. The total evapotranspiration according to the Penman – Monteith – Leuning model, and its components – heat energy flows measured by remote sensing data – was actually investigated.

#### **Analysis of recent research and publications.**

Evapotranspiration indicators are defined at the global level for the Earth’s surface areas based on the Penman – Monteith – Leuning (PML) dataset of the second version (V2) according to Zhang [1]. Evapotranspiration (ET) in the “soil-plant-atmosphere” system includes direct evaporation from the soil ( $E_s$ ), transpiration from vegetation ( $E_c$ ), and evaporation of intercepted precipitation

from vegetation ( $E_i$ ), i.e. the moisture that has evaporated from the moistened plant surface (leaves). ET is the main pathway for returning water to the atmosphere and plays a key role in the water-energy-carbon cycle [12]. ET is an important component in water resources management, drought monitoring, water accounting, the assessment of water productivity and global climate change. Separating ET components into  $E_s$ ,  $E_c$ , and  $E_i$  can improve understanding of the global interaction between terrestrial ecosystems and the atmosphere [13].

The assessment of the accuracy of evapotranspiration (ET) measurement methods using remote sensing data, in particular the Penman – Monteith method in irrigated areas, was carried out using the RS-PML (Remote Sensing Penman – Monteith – Leuning) model. This study included irrigated vineyards, which are difficult to analyze due to the impact on microclimate and water resource requirements [8]. RS-PM models were found to show higher accuracy compared to other models, such as METRIC and TSEB-PT (Sebal), at different time scales, including instantaneous, daily, weekly, and seasonal ones. The root mean square error (RMSE) for RS-PM models was the lowest and amounted up to 23 % [8]. This highlights the significant advantages of RS-PM models on irrigated areas.

The RS-PMS algorithm, which is based on the combination of RS-PM with the Stewart stomatal conduction model, deserves special attention when assessing accuracy. This algorithm provided the highest accuracy among all the models analyzed achieving an RMSE of 19 %. However, spatial extension of this model requires adaptation to individual conditions, including crop and regional peculiarities, as well as an increase in the number of input parameters, such as local climate data, soil type, and irrigation practices [8]. This demonstrates the potential of RS-PMS for more accurate evapotranspiration forecasting, but also indicates the difficulty of its implementation at the global scale.

Analysis of seasonal variations of evapotranspiration (ET) components showed that they are significantly correlated with major meteorological variables such as air temperature, relative humidity, and precipitation. However, the ratio of ET components has been shown to be more dependent on irrigation practices, water management methods, and other local conditions than on general meteorological variables [14]. This means that successful application of ET measurement models requires a comprehensive approach that takes into account both climatic factors and agronomic practices.

To test the accuracy of global evapotranspiration models, the researchers used the global PML-V2 product, which was calibrated based on observations from eddy covariance stations located in China covering nine functionally different vegetation types. The results showed that the global model performs well in cross-validation mode, confirming its high accuracy. In addition, more accurate evapotranspiration models were developed for the territory of China using PML-V2 compared to previous versions [15–16], which was made possible by increasing the frequency of receiving input parameters, such as daily (instead of 8-day) satellite data of better detailing for determining evapotranspiration. This allowed, in addition to calculating the dynamics of evapotranspiration, to determine arable fields with a double crop system, which contributes to more accurate measurement of ET in agricultural areas [12]. Verification of the proposed model in Ukrainian conditions has not yet been carried out.

Publications indicate active development of research in the field of using new high-resolution data on evapotranspiration and vegetation productivity (GPP models). Also, extensive cloud environments with a large number of satellite images are becoming the basis for real-time monitoring of water resources. These technologies are actively used by researchers in collaboration with water and environmental departments in various countries around the world to manage water resources, assess climate change, and the impact of agronomic practices on ecosystems.

**The aim of the research.** Determination of the evapotranspiration components' spatial distribution, analysis of its dynamics in different agro-climatic zones based on remote sensing data with the use of PML-V2 model algorithms, cloud servers, and the developed software.

**Materials and research methods.** Obtaining accurate knowledge of actual evapotranspiration (ET) and its components with high resolution is critically important for understanding the dynamics of processes in the “soil-plant-atmosphere” system. To carry out this study, a method of evapotranspiration calculation based on the analysis of a series of satellite images and digital data sets was chosen. In particular, the Penman – Monteith – Leuning model (abbreviated as PML-V1 and PML-V2) was used. This model was proposed by Leuning in 2008 [9], and also improved by Zhang in 2010, 2016, and 2019 [17–18]. Based on the set of initial data, using the algorithms of the PML model [19], evaporation and its components were determined,

namely transpiration from vegetation ( $E_c$ ), direct evaporation from soil ( $E_s$ ), evaporation of intercepted precipitation from vegetation ( $E_i$ ), and its spatial distribution over the territory of Ukraine.

The PML-V2 model uses total primary productivity and atmospheric  $\text{CO}_2$  concentration to estimate the conductivity of the study surface, thus establishing a relationship and jointly estimating ET and total primary productivity. ET in this study is obtained separating it into three main components: vegetation transpiration ( $E_c$ ), soil evaporation ( $E_s$ ), and precipitation evaporation intercepted by plants ( $E_i$ ), which are calculated as follows [1, 14].

$$ET = E_c + E_s + E_i, \quad (1)$$

$$E_c = \frac{\varepsilon A_c + \left( \frac{\rho C_p}{\gamma} \right) D_a G_a}{\varepsilon + 1 + \frac{G_a}{G_c}}, \quad (2)$$

$$E_s = \frac{f \varepsilon A_s}{\varepsilon + 1}, \quad (3)$$

$$E_i = \begin{cases} f_v PP < P_{wet} \\ f_v P_{wet} + f_v (P - P_{wet}) P \gg P_{wet} \end{cases}, \quad (4)$$

where  $\varepsilon = s/\gamma$ ,  $\gamma$  is the psychrometric constant ( $\text{kPa}/^\circ\text{C}$ ),  $s$  is the the slope of the curve, which is the ratio of water vapor pressure at saturation point to the temperature ( $\text{kPa}/^\circ\text{C}$ );  $A$  is the available energy absorbed by the surface ( $\text{MJ}/(\text{m}^2 \text{ per day})$ ), i.e. net absorbed radiation minus soil heat flux;  $A_s$  and  $A_c$  are the available energy of soil and vegetation cover respectively;  $\rho$  is the air density ( $\text{g}/\text{m}^3$ );  $C_p$  is the specific heat capacity of air at constant pressure ( $\text{MJ}/(\text{g}^\circ\text{C})$ );  $D_a$  is the air water vapor pressure deficit ( $\text{kPa}$ );  $C_a$  is the aerodynamic conductivity ( $\text{m}/\text{s}$ );  $G_c$  ( $\text{m}/\text{s}$ ) is the plant surface conductivity, which is a function of atmospheric carbon dioxide ( $\text{CO}_2$ ) concentration, pressure, and water vapor pressure deficit;  $f$  is the dimensionless variable that determines the availability of water for evaporation from the soil;  $f_v$  is the leaf area of the studied surface;  $P$  is the daily precipitation ( $\text{mm}/\text{day}$ );  $P_{wet}$  is the precipitation threshold when the studied surface is sufficiently wet.

To obtain spatial assessment and analysis of distribution results, special software was developed, namely scripts using the JavaScript programming language for remote data processing using the cloud software environment in the Google Earth Engine (GEE) [20]. This software allows to customize the PML model for Ukrainian conditions and visualize the spatial distribution of ET.

The calculation of evapotranspiration and its components is carried out using the formulas (1–4) on GEE servers for the entire Earth’s surface. The input data for further processing is available through the developed user interface and is an ImageCollection object. The model code is publicly available and is distributed under the GPLv2 license [21]. The model is accessed by

executing user requests on the GEE server. The result of the analysis of the territory in our study according to the Penman – Monteith – Leuning model is a composite mosaic, that is a generalized image of the territory with detailing at the selected points [22]. The flowchart of the implementation of the Penman–Monteith–Leuning model in GEE is shown in Figure 1 [21].

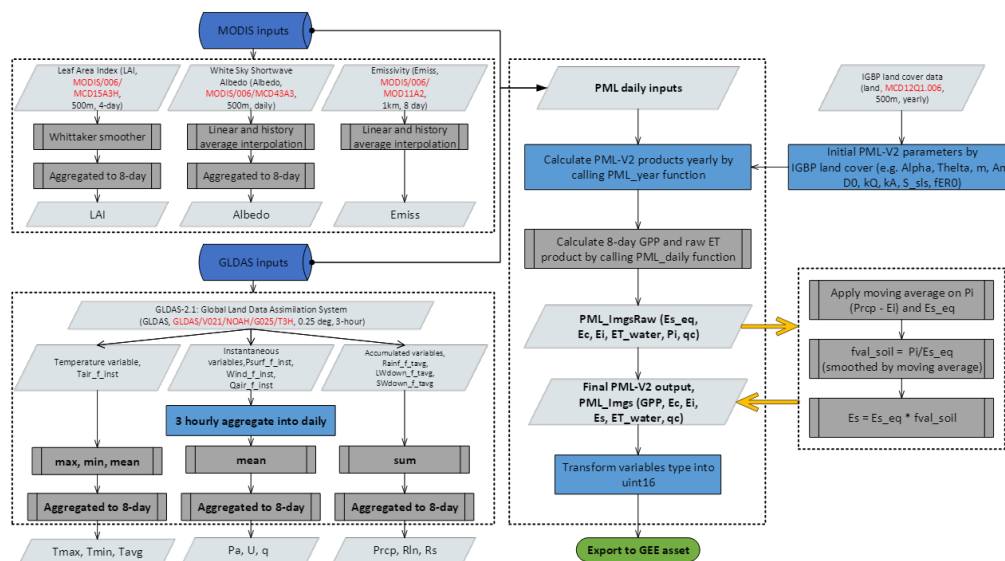


Fig. 1. Flowchart of the implementation of the Penman–Monteith–Leuning model in the Google Earth Engine

The usage of the service’s cloud capabilities allowed to access the collection of images and perform their remote processing using the Penman – Monteith – Leuning algorithm, which is calibrated using the towers of the global network of eddy covariance observation stations on the base of a territory mask. The result of the assessment is a spatially distributed generalized image of evapotranspiration and its components over the territory of Ukraine.

The PML model uses 500 m resolution of MODIS for data regarding leaves, albedo, and surface emissivity, as well as meteorological data coming from the Global Land Data Assimilation System (GLDAS) version 2. GLDAS receives observational data from both satellites and ground-based sources on temperature variability, instantaneous pressure, wind speed, and relative humidity, as well as total daily precipitation, long- and short-wave solar radiation. Using modern methods of Earth surface modeling and data assimilation, the GLDAS system generates optimal fields of Earth surface states and flows. The GLDAS 2 input data has a spatial resolution of 0.25° (~25 km), which is interpolated to

the 500-meter grid of the PML dataset [21]. Evapotranspiration is calculated once per every 8 days, the calculation components are measured at 3-hour intervals and aggregated into 1-day and 8-day values (Fig. 1).

To analyze the distribution of evapotranspiration components, territories, on which the intensity of evapotranspiration was the same, were initially identified based on remote sensing data. For agro-climatic zones on the maps, these territories were identified in an independent manner. In different zones (Fig. 2) reference points were selected in the form of three plots of 0.25 km<sup>2</sup> each, namely the territory in the Steppe zone under irrigation (Kherson region), in the Forest-Steppe – agricultural fields (Cherkasy region), and Polissya – reclaimed forests (Volyn region) for the growing season of 2020, when the irrigation systems of southern Ukraine worked intensively.

The distribution of evapotranspiration components, which depends on applied agricultural practices, was clarified on the plots. That is, an analysis on the amount of moisture evaporating from the open soil



surface, transpiration of moisture by plants, and evaporation directly from the leaf surface was conducted. Thus, on each of the plots of

preliminary studies, we tested the hypothesis regarding the dynamics of the ET components distribution.

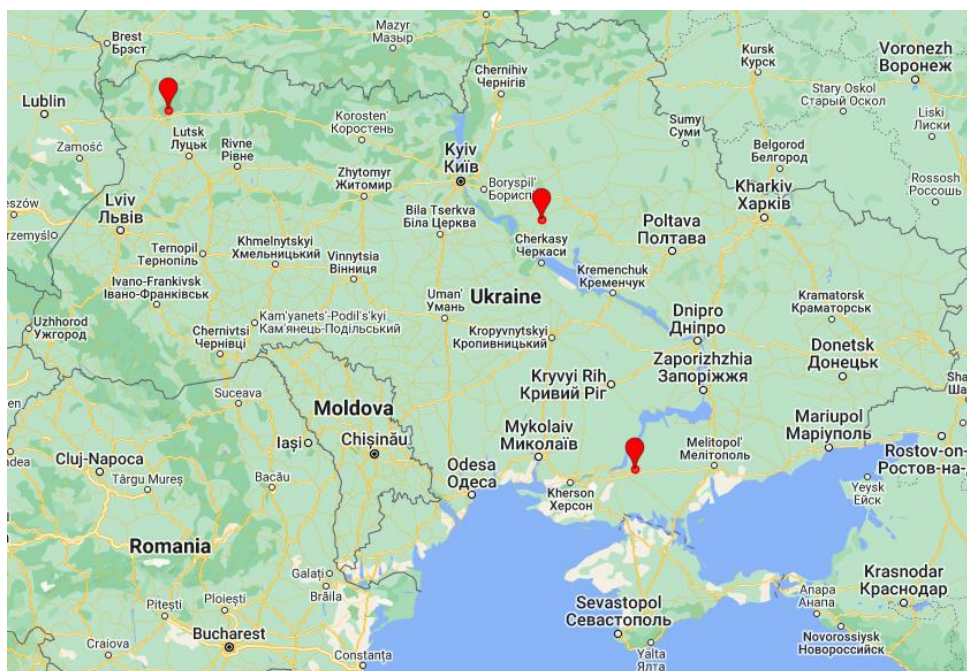


Fig. 2. Locations of the studied plots for different agro-climatic zones of Ukraine (Steppe, Forest-Steppe, Polissya)

### Research results and their discussion.

To determine and assess the state of available water resources, effectively implement climate change adaptation strategies, the determination of the components of the water balance is a key element of effective water resources management. Evapotranspiration is the main and the most important component in the water cycle. In the study, the  $E_c$  component of the split evapotranspiration flux is estimated to assess the actual water consumption by plants at the country level. The  $E_i$  component is used to assess the effectiveness of precipitation, and the  $E_s$  component is used to assess soil moisture and the shading degree. Generalized images – the maps of the spatial distribution of evapotranspiration components – were obtained (Fig. 3). The scale was chosen to visualize the differentiation of evapotranspiration components. Within the territory of Ukraine, some of the maximum values are deliberately excluded and are not represented on the palette to increase the contrast of the average seasonal values visualization. That is, the maximum values in the case of visual assessment, e.g. of  $E_s$ , are 0.6 mm/day and above.

The soil evaporation distribution map ( $E_s$ ) represents the moisture evaporation from the open soil surface and depends on the availability of soil moisture, the degree of surface shading by vegetation, and the deficit of atmospheric moisture. The spatial distribution of  $E_s$  reflects the regions of the country, in which the soil loses moisture most intensively through evaporation from the open soil surface (Fig. 3a). The Steppe and Forest-Steppe regions have the highest evaporation intensity values.

The map of distribution of the evaporation of precipitation retained by vegetation is used to estimate the fraction of precipitation that goes to evapotranspiration. This component depends on the amount of precipitation and the vegetation cover particularities. The spatial distribution of  $E_i$  shows how efficiently precipitation is used by plants in different zones (Fig. 3b). This indicator reaches its highest value in the regions densely covered with vegetation.

The vegetation transpiration distribution map ( $E_c$ ) determines the dynamic flow of  $E_c$ . The map represents the agro-climatic zones that have the highest or the lowest rates of plants' water use, which is critical for water management in agriculture.

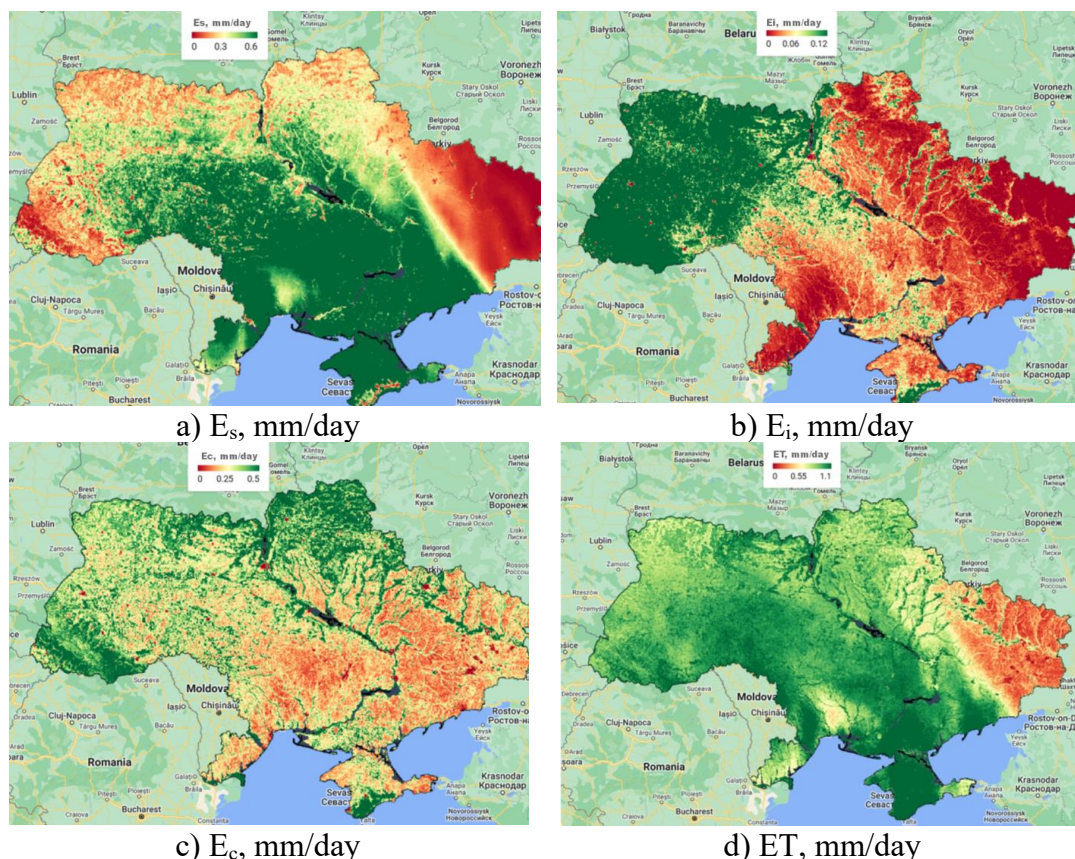


Fig. 3. Maps of the distribution of the evapotranspiration components intensity for the growing season of 2020 (01.04.20–30.09.20)

Thus, the distribution map of the total average intensity of evapotranspiration identifies agroclimatic zones with increased evapotranspiration, which in the obtained results coincide with the regions where negative trends in the availability of water resources for plants are observed (Fig. 3d).

Daily evapotranspiration values were studied on individual images and presented as a series of observations visualized in the form of histograms and maps of evapotranspiration

spatial distribution and stored in database tables. Figure 4a shows the distribution of global maximum and minimum values based on minimax analysis across the country in the form of histograms, which corresponds to daily ET estimated using the PML model. For example, as of July 3, 2020, the maximum recorded ET value from the water surface is 8.5 mm, the maximum evapotranspiration from the land surface is 4.13 mm, while the minimum value is 2.43 mm.

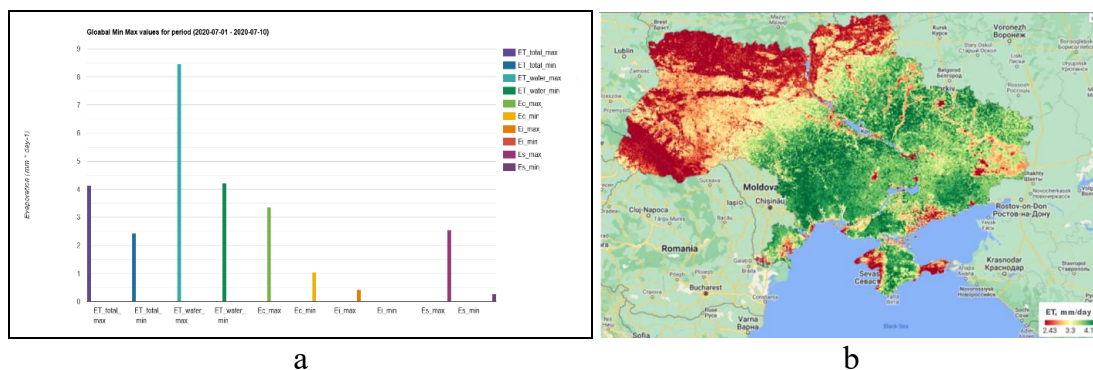


Fig. 4. Spatial distribution of absolute values of evapotranspiration in the form of a histogram and a map for 03.07.2024



It is important to mention that the studied plot of 0.25 km<sup>2</sup> includes various topographic elements, for example, the Steppe zone area may include both irrigated and non-irrigated areas (field roads, roadsides, etc.), since the pixel of the satellite image does not always fall completely within the boundaries of the field. The actual flow from this plot reflects both the evapotranspiration data of an individual monoculture and all adjacent areas included in the observation zone.

By analyzing the distribution of components in different agro-climatic zones, it was determined that in each zone the percentage of the contribution from each component to the total evapotranspiration is different. The absolute value of total transpiration during the season also differs. So, in the Steppe 60 % of ET is the transpiration from plants, in the Forest-Steppe this component amounts to 66 %, and in the Polissya zone – to 65 %. However, the largest difference in percentage between zones has the evaporation of precipitation retained by vegetation. In the Steppe zone it only amounts to 2 %, while in the Polissya its share is 24 % (Fig. 5).

The dynamic values of  $E_s$ ,  $E_c$ ,  $E_i$  from remote sensing maps are accumulated in the form of daily data tables and form a static value of the number of

mm evaporated from the studied pixel of 0.25 km<sup>2</sup> plot during the season. Data on absolute and percentage distribution are given in Table 1.

1. Total ET values for the season and its components distribution in absolute and percentage forms during the growing season.

Component	Steppe		Polissia		Forest-Steppe	
	mm	%	mm	%	mm	%
$E_c$	269,68	60	216,96	65	302,24	66
$E_i$	10,80	2	78,00	23	18,00	4
$E_s$	170,24	38	36,96	11	136,96	30
ET	450,72	100	331,92	100	457,20	100

The dynamics of evapotranspiration components during the growing season also varies depending on the selected agro-climatic zone (Figure 6).

A feature of the distribution dynamics for reclaimed areas of the Steppe with early vegetation restoration is a representative reduction of the evaporation from the open soil surface at the beginning of the season and its increase in the middle, after the end of the active agricultural crops' vegetation and early harvest of

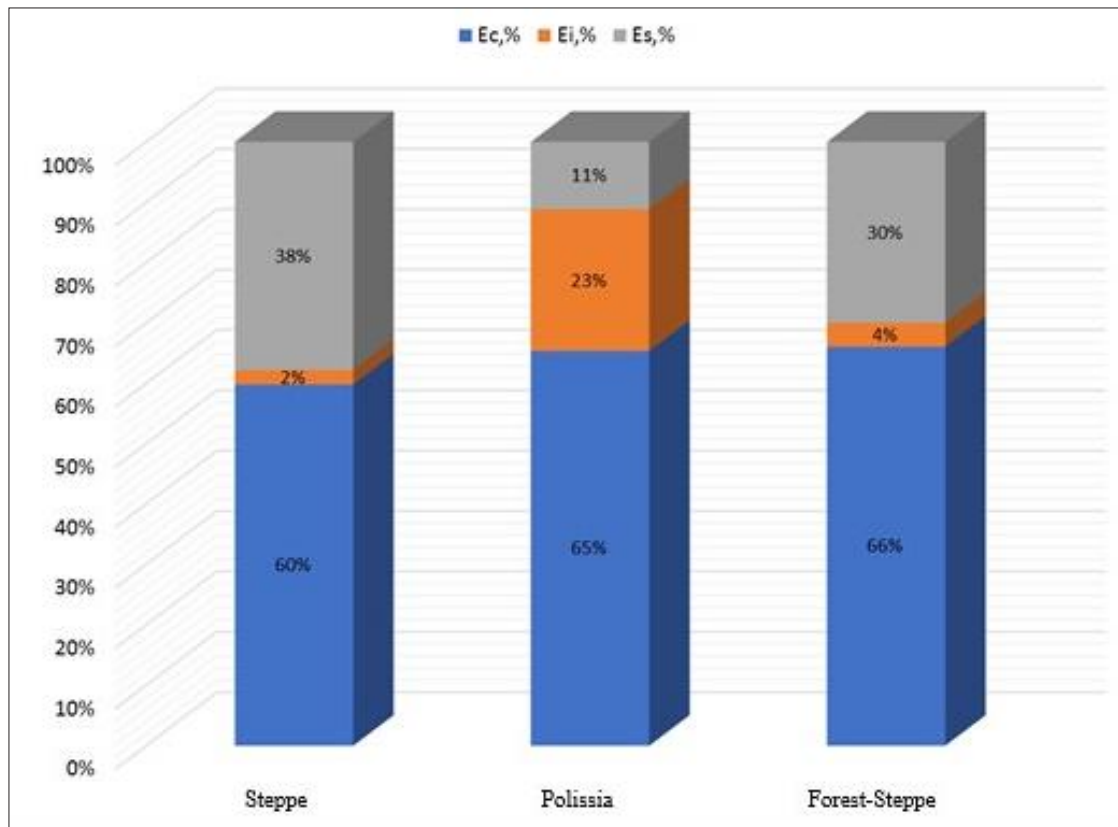
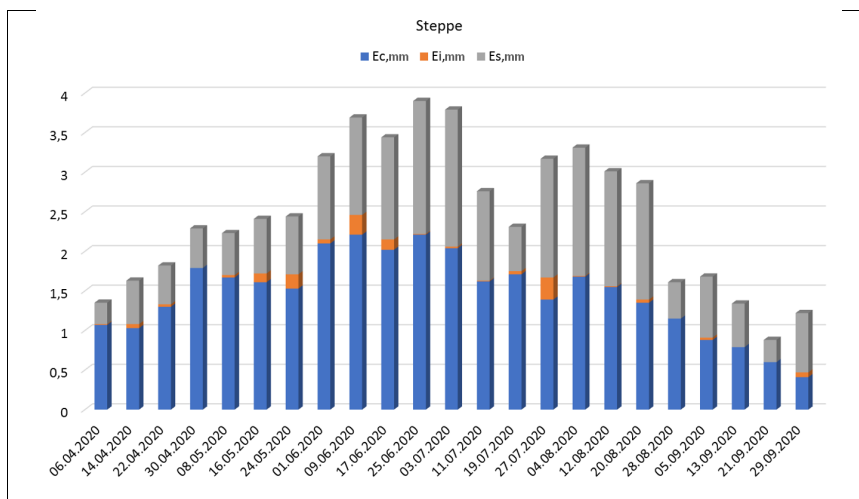
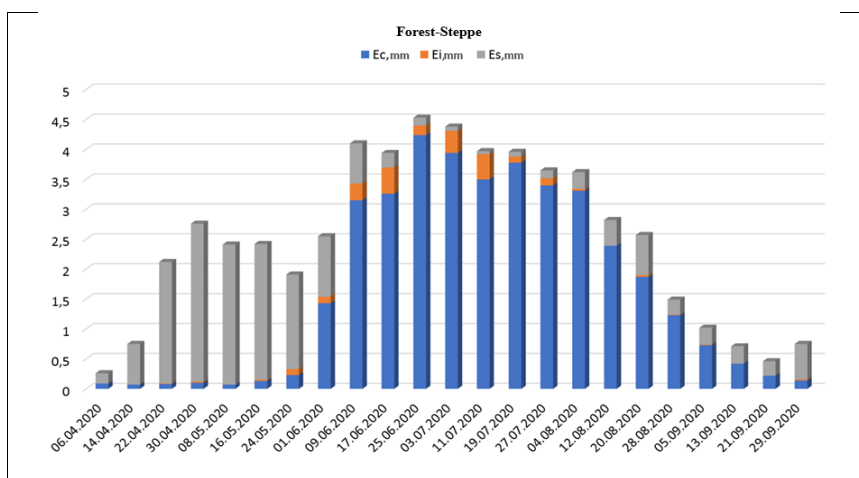


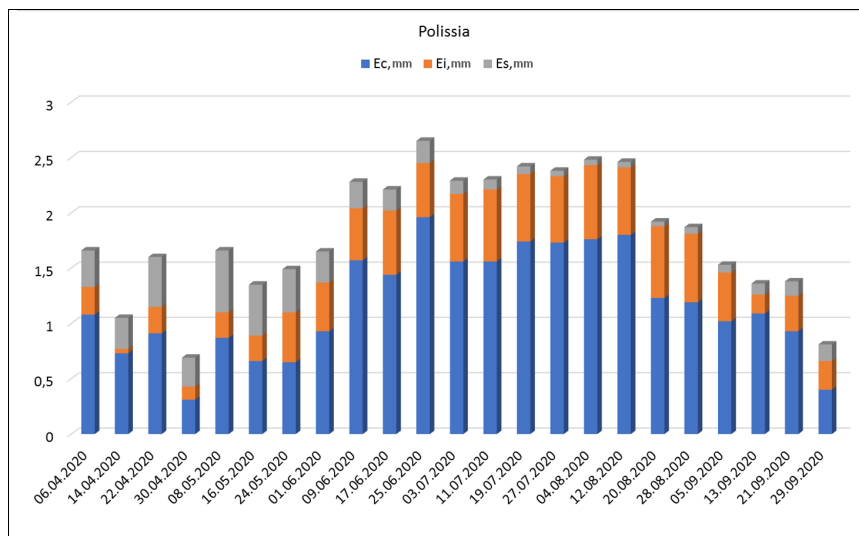
Fig. 5. Seasonal distribution of evapotranspiration components in different agro-climatic zones of Ukraine during the 2020 growing season (01.04.20–30.09.20)



a) Dynamics of the distribution of evapotranspiration and its components during the 2020 growing season in the Steppe zone



b) Dynamics of the distribution of evapotranspiration and its components during the 2020 growing season in the Forest-Steppe zone



c) Dynamics of the distribution of evapotranspiration and its components during the 2020 growing season in the Polissya zone

Fig. 6. Dynamics of the distribution of evapotranspiration and its components during the 2020 growing season in different agro-climatic zones of Ukraine



cereals (Fig. 6a). The value of evapotranspiration of a selected plot will depend significantly on the irrigation technologies used by the farm. In the 2020 growing season, evapotranspiration in the Steppe zone according to the remote sensing data (daily values were observed within the range of 3,83–5,12 mm) indicates insufficient water in the soil to fully cover the moisture deficit.

Figure 6b characterizes the areas with complete turning over of the arable soil layer, therefore, in the dynamics at the beginning of the growing season, evaporation from the open soil prevails, but after that it decreases with the development of vegetation cover. Figure 6c characterizes the territories of the Polissya with reclaimed forests. In the dynamics of the distribution of total evapotranspiration, compared to the other regions, evaporation from the surface of plants prevails and the evaporation of precipitation intercepted by vegetation is also noticeably present. Since the soil is covered with a layer of plant residues, evaporation from the open surface is smaller.

The algorithm and the applied model for obtaining estimates of ET and its components showed the distribution of evapotranspiration and its components in different agro-climatic zones on a regional scale. To obtain more detailed maps of the distribution, more detailed remote sensing data is needed and further cross-validation of the model using eddy covariance towers is possible. Further research will focus on determining the relationship between evapotranspiration and its components with gross primary production and on verifying the model in Ukrainian conditions.

### Conclusions.

1. The implemented algorithm based on the use of remote sensing data effectively performs spatial estimation of evapotranspiration (ET) and its components based on the improved Penman – Monteith – Leuning method. The use of remote sensing data provides an opportunity to perform detailed ET modeling over large areas with high resolution, which contributes to the optimization of water use processes.

2. The possibility of using geospatial datasets from remote servers for spatial assessment of evapotranspiration and its components

using software developed by the authors has been proven. A software product has been developed to analyze the spatial distribution of evapotranspiration components in different agro-climatic zones. The program code is located in the Google Earth Engine repository and is constantly being improved both by the team of authors of the article, who develop applied technologies for using remote sensing data for assessment, and by the providers of the datasets.

3. The resulting generalized images and geospatial maps of evapotranspiration components based on remote sensing data are an important tool for water resources management. Visualization of the dynamics of evapotranspiration processes allows making justified decisions regarding water supply management in different agro-climatic zones taking into account local natural conditions. This is especially important for the water-scarce zones, where evapotranspiration control can ensure efficient water use and prevent losses due to inefficient irrigation and tillage technologies.

4. Models, which are using remote sensing data for estimating evapotranspiration dynamics, require additional validation and comparison with actual field measurements. Quantitative indicators obtained through the modeling should be coordinated with the data from ground-based stations of the greenhouse gas fluxes monitoring to improve the forecasts accuracy and to identify possible deviations. This will ensure further improvement of the methodology and facilitate its adaptation to the conditions of different agricultural regions.

5. The use of maps of geospatial distribution of evapotranspiration over Ukraine based on global data allows identifying regions with higher transpiration and a potential shortage of available water resources. These maps are a valuable tool for forecasting the availability and for planning of the usage of water resources, which is critically important for the agricultural sector. Identification of the such zones will help introduce the preventive measures to improve water availability, implement effective irrigation methods, and preserve agricultural crops in arid conditions.

### References

1. Zhang, Y., Kong, D., Gan, R., Chiew, F. H. S., McVicar, T. R., Zhang, Q., & Yang, Y. (2019). Coupled estimation of 500 m and 8-day resolution global evapotranspiration and gross primary production in 2002–2017. *Remote Sensing of Environment*, 222, 165–182. DOI: <https://doi.org/10.1016/j.rse.2018.12.031>
2. Ji, Y., Tang, Q., Yan, L., Wu, S., Yan, L., Tan, D., Chen, J., & Chen, Q. (2021). Spatiotemporal variations and influencing factors of terrestrial evapotranspiration and its components during different impoundment periods in the Three Gorges Reservoir area. *Water*, 13 (15), 2111. DOI: <https://doi.org/10.3390/w13152111>

3. Ma, L., Li, Y., Wu, P., Zhao, X., Chen, X., & Gao, X. (2020). Coupling evapotranspiration partitioning with water migration to identify the water consumption characteristics of wheat and maize in an intercropping system. *Agricultural and Forest Meteorology*, 290, 108034. DOI: <https://doi.org/10.1016/j.agrformet.2020.108034>
4. Valentín, F., Nortes, P. A., Domínguez, A., Sánchez, J. M., Intrigliolo, D. S., Alarcón, J. J., & López-Urrea, R. (2020). Comparing evapotranspiration and yield performance of maize under sprinkler, superficial and subsurface drip irrigation in a semi-arid environment. *Irrigation Science*, 38, 105–115. <https://doi.org/10.1007/s00271-019-00654-7>
5. Jiao, L., Lu, N., Fu, B., Wang, J., Li, Z., Fang, W., Liu, J., Wang, C., & Zhang, L. (2018). Evapotranspiration partitioning and its implications for plant water use strategy: Evidence from a black locust plantation in the semi-arid Loess Plateau, China. *Forest Ecology and Management*, 424, 428–438. DOI: <https://doi.org/10.1016/j.foreco.2018.05.006>
6. Paredes, P., Rodrigues, G. C., Alves, I., & Pereira, L. S. (2014). Partitioning evapotranspiration, yield prediction and economic returns of maize under various irrigation management strategies. *Agricultural Water Management*, 135, 27–39. DOI: <https://doi.org/10.1016/j.agwat.2014.01.013>
7. Gong, X., Qiu, R., Ge, J., Bo, G., Ping, Y., Xin, Q., & Wang, S. (2021). Evapotranspiration partitioning of greenhouse-grown tomato using a modified Priestley–Taylor model. *Agricultural Water Management*, 247, 106709. DOI: <https://doi.org/10.1016/j.agwat.2020.106709>
8. García-Gutiérrez, V., Stöckle, C., Gil, P. M., & Meza, F. J. (2021). Evaluation of Penman – Monteith model based on Sentinel-2 data for the estimation of actual evapotranspiration in vineyards. *Remote Sensing*, 13 (3), 478.
9. Leuning, R., Zhang, Y. Q., Rajaud, A., Cleugh, H., & Tu, K. (2008). A simple surface conductance model to estimate regional evaporation using MODIS leaf area index and the Penman – Monteith equation. *Water Resources Research*, 44, W10419. DOI: <https://doi.org/10.1029/2007WR006562>
10. Kang, W., Ni, F., Deng, Y., Xiang, J., Yue, Z., Wu, M., & Jiang, N. (2024). Drought impacts on blue and green water: A spatial and temporal analysis. *Ecological Indicators*, 158, 111319.
11. Lowe, B. H., Zimmer, Y., & Oglethorpe, D. R. (2022). Estimating the economic value of green water as an approach to foster the virtual green-water trade. *Ecological Indicators*, 136, 108632.
12. He, S., Zhang, Y., Ma, N., Tian, J., Kong, D., & Liu, C. (2022). A daily and 500 m coupled evapotranspiration and gross primary production product across China during 2000–2020. *Earth System Science Data*, 14 (12), 5463–5488. DOI: <https://doi.org/10.5194/essd-14-5463-2022>
13. Xu, F., Wang, W., Wang, J., Xu, Z., Qi, Y., & Wu, Y. (2017). Area-averaged evapotranspiration over a heterogeneous land surface: Aggregation of multi-point EC flux measurements with a high-resolution land-cover map and footprint analysis. *Hydrology and Earth System Sciences*, 21, 4037–4051. DOI: <https://doi.org/10.5194/hess-21-4037-2017>
14. Chen, J., Tan, H., Ji, Y., Tang, Q., Yan, L., Chen, Q., & Tan, D. (2021). Evapotranspiration Components Dynamic of Highland Barley Using PML ET Product in Tibet. *Remote Sensing*, 13 (23), 4884.
15. Laipelt, L., Kayser, R. H. B., Fleischmann, A. S., Ruhoff, A., Bastiaanssen, W., Erickson, T. A., & Melton, F. (2021). Long-term monitoring of evapotranspiration using the SEBAL algorithm and Google Earth Engine cloud computing. *ISPRS Journal of Photogrammetry and Remote Sensing*, 178, 81–96.
16. Laipelt, L., Rossi, J. B., de Andrade, B. C., Scherer-Warren, M., & Ruhoff, A. (2024). Assessing Evapotranspiration Changes in Response to Cropland Expansion in Tropical Climates. *Remote Sensing*, 16 (18), 3404.
17. Zhang, Y., Peña-Arancibia, J. L., McVicar, T. R., Chiew, F. H. S., Vaze, J., Liu, C., Lu, X., Zheng, H., Wang, Y., Liu, Y. Y., & Miralles, D. G. (2016). Multi-decadal trends in global terrestrial evapotranspiration and its components. *Scientific Reports*, 6, 19124. DOI: <https://doi.org/10.1038/srep19124>
18. Gan, R., Zhang, Y. Q., Shi, H., Yang, Y. T., Eamus, D., Cheng, L., Chiew, F. H. S., & Yu, Q. (2018). Use of satellite leaf area index to estimate evapotranspiration and gross assimilation for Australian ecosystems. *Ecohydrology*. DOI: <https://doi.org/10.1002/eco.1974>
19. Google Developers. (n.d.). CAS\_IGSNRR\_PML\_V2\_v017 dataset. (дата звернення 5.10.2024), Retrieved from: [https://developers.google.com/earth-engine/datasets/catalog/CAS\\_IGSNRR\\_PML\\_V2\\_v017](https://developers.google.com/earth-engine/datasets/catalog/CAS_IGSNRR_PML_V2_v017)
20. Google Earth Engine. (n.d.). Retrieved from: <https://earthengine.google.com/>

21. GitHub. (n.d.). gee\_PML repository. Retrieved from: [https://github.com/gee-hydro/gee\\_PML](https://github.com/gee-hydro/gee_PML)
22. Google Developers. (n.d.). PML\_V2: Coupled Evapotranspiration and Gross Primary Product dataset. Retrieved from: [https://developers.google.com/earth-engine/datasets/catalog/CAS\\_IGSNRR\\_PML\\_V2](https://developers.google.com/earth-engine/datasets/catalog/CAS_IGSNRR_PML_V2)

УДК 631.67:004

## ОЦІНКА ДИНАМІКИ КОМПОНЕНТІВ ЕВАПОТРАНСPIРАЦІЇ В РІЗНИХ АГРОКЛІМАТИЧНИХ ЗОНАХ УКРАЇНИ З ВИКОРИСТАННЯМ МОДЕЛІ ПЕНМАНА – МОНТЕЙТА – ЛЕУНІНГА

**Т.В. Матяш<sup>1</sup>**, канд. техн. наук, **Я.О. Бутенко<sup>2</sup>**, канд. с.-г. наук, **А.М. Смірнов<sup>3</sup>**, аспірант,  
**Є.І. Матяш<sup>4</sup>**, магістр

<sup>1</sup> Інститут водних проблем і меліорації НААН, Київ, Україна;

<https://orcid.org/0000-0003-1225-086X>; e-mail: [t.v.matiash@gmail.com](mailto:t.v.matiash@gmail.com)

<sup>2</sup> Інститут водних проблем і меліорації НААН, Київ, Україна;

<https://orcid.org/0000-0002-1743-7175>; e-mail: [iarynabulba@gmail.com](mailto:iarynabulba@gmail.com)

<sup>3</sup> Інститут водних проблем і меліорації НААН, Київ, Україна;

<https://orcid.org/0009-0006-5865-9141>; e-mail: [justtosha@gmail.com](mailto:justtosha@gmail.com)

<sup>4</sup> НТУУ «Київський політехнічний інститут імені Ігоря Сікорського», Київ, Україна;

<https://orcid.org/0009-0007-7079-3017>; e-mail: [liza.mymailbox@gmail.com](mailto:liza.mymailbox@gmail.com)

**Анотація.** У статті проаналізовано результати оцінки евапотранспірації (ЕТ) та її компонентів за даними дистанційного зондування Землі. Для отримання цієї оцінки було розроблено спеціальне програмне забезпечення, а саме скрипти з використанням мови програмування JavaScript для віддаленої обробки даних у хмарному програмному середовищі Google Earth Engine (GEE). Це програмне забезпечення дозволяє налаштувати для умов України модель Пенмана – Монтейта – Леунінга (PML) та візуалізувати просторовий розподіл ЕТ. Використання хмарних можливостей сервісу дозволило отримати доступ до колекції знімків та проводити віддалену їх обробку за алгоритмом Пенмана – Монтейта – Леунінга, що відкалібрований за даними світової мережі станцій спостереження вихрової коваріації. Результатом такої оцінки стала композитна мозаїка – просторово розподілене узагальнене зображення евапотранспірації та її трьох основних компонентів: транспірацію з рослинності ( $E_c$ ), випаровування з ґрунту ( $E_s$ ) і випаровування перехоплених опадів рослинним покривом ( $E_i$ ) на території України за вегетаційний сезон 2020 року. Розуміння динаміки цих компонентів сприяє оптимізації використання водних ресурсів та розробці ефективних схем зрошення, особливо в умовах змін клімату. В результаті аналізу динаміки складових евапотранспірації протягом вегетаційного сезону здійснено визначення найбільш вагомого компоненту евапотранспірації у різних агрокліматичних зонах.

Проте моделі, що використовують дистанційні дані для оцінки динаміки евапотранспірації, вимагають додаткової валідації та порівняння з польовими вимірюваннями для підвищення їхньої точності. Кількісні показники, отримані через моделювання, повинні узгоджуватися з даними наземних станцій моніторингу потоків парникових газів, що сприятиме вдосконаленню методології та адаптації її до умов різних аграрних регіонів. Окрім того, використання карт геопросторового розподілу евапотранспірації дозволяє ідентифікувати регіони з підвищеною транспірацією та потенційним дефіцитом водних ресурсів. Такі карти стають цінним інструментом для планування і прогнозування водних ресурсів, що є критично важливим для аграрного сектору.

**Ключові слова:** евапотранспірація, компоненти евапотранспірації, агрокліматичні зони, дистанційне зондування Землі, ґрунт-рослина-атмосфера, інформаційна система, модель Пенмана – Монтейта – Леунінга, PML-V2, GEE програмування